Journal of Research of the National Bureau of Standards Vol. 55, No. 6, December 1955 Research Paper 2640

Reflection and Transmission of Gamma Radiation by Barriers: Monte Carlo Calculation by a Collision-Density Method [1, 2]

Martin J. Berger

The collision density of photons in an infinite Compton-scattering medium was calculated by random sampling. The intensity, spectral composition, and angular distribution were then determined for radiation reflected and transmitted by plane-parallel barriers by carrying out appropriate integrations over the collision density, taking into account the absorbing properties of the medium and the effect of boundaries. All numerical work was done on the National Bureau of Standards automatic computer (SEAC). Sample results are presented for 0.66-Mev radiation incident on water barriers of various thicknesses.

1. Introduction

The Problem. The results of an investigation of the following boundary problem in gamma-ray diffusion are presented: A beam of monoenergetic gamma rays is incident at a given angle on a plane-parallel barrier that has a finite thickness in one dimension but is infinite in the other two dimensions. What are the intensities and spectral compositions of the reflected and transmitted beam?

Method of Solution. An analytical attack on this problem by the solution of the relevant transport equation leads to great mathematical difficulty. So far such an approach has been successfully carried out for homogenous infinitely extended media [1],[3] but boundary problems remain unsolved. In order to bypass these difficulties, explore the problem, and obtain at least an approximate solution, this investigation employed the Monte Carlo (random sampling) method. All numerical work was carried out on the automatic computer of the National Bureau of Standards (SEAC).

The calculation was divided, in regard to both method and execution, into two rather distinct parts: (1) a stochastic part, in which photon random walks are generated by random sampling in an infinite nonabsorbing scatterer, whereby a collision density is obtained, and (2) a calculation of the reflected and transmitted radiation obtained by summations over collision densities, taking into account boundary conditions and absorption characteristics of the barrier. There were a number of reasons for this division. For one thing, it reduced the required computer memory capacity. More importantly, the random walks have a "universal" character, i. e., they can be used for the calculation of different boundary problems involving different geometries as well as different scattering and absorbing media. Not only will the repeated use of the same set of random walks often lead to computing economy, but it may also increase the accuracy of a calculation. Suppose, for example, that we wish to determine the difference in transmission for two beams incident on a barrier at different angles but otherwise identical. It will then be to our advantage to base the comparison on the same set of random walks because irrelevant differences resulting from statistical fluctuations will thereby be largely eliminated.

2. Gamma-Ray Random Walks in an Infinite Compton Scatterer

2.1. Definitions

The state S of a photon can be specified by a set of six quantities:

$$S=(E,\theta,\varphi,x,y,z),$$

where E is the photon energy, θ and φ are angular coordinates describing the direction of motion (in a spherical coordinate system with the z-axis as polar axis), and x, y, and z are Cartesian coordinates of position. Let the state of the photon immediately after the nth scattering event occurring in a given random walk be denoted by $S_n (n=1,2,\cdots)$, and let S_0 denote the state in which it was introduced into the scattering medium. A random walk is then described by a sequence

$$S_0,\ S_1,\ S_2,\ \cdots,\ S_L,$$

each term (except S_0) depending stochastically on its immediate predecessor only (Markov process). The length, L, of such a sequence would be infinite, but in the present work the random walks are terminated when the energy, E, drops below 30 kev. This arbitrary cutoff [4] results in an average value $\langle L\rangle=18$ for an initial energy $E_0=660$ kev. A

[1] This work was supported by the Office of Naval Research and the Atomic Energy Commission Reactor Division.

[2] Some of the results of this paper were presented at a symposium on Monte Carlo methods at the University of Florida in March 1954.

[3] Figures in brackets indicate the literature references at the end of this paper.

[4] The cutoff is justified on physical grounds because radiation at energies below 30 kev is always so heavily absorbed that it makes only a negligible contribution to the emergent radiation flux.

set of random walks constitutes a Monte Carlo estimate of the collision density resulting from the diffusion of radiation in an infinite homogenous Compton scatterer.

It will be observed that for the problem of transmission and reflection by plane-parallel barriers, only the variables E, θ and one space variable, say z, are required. Nevertheless, it is worthwhile to calculate the other three variables also. The random walks are thus made applicable to other boundary problems with different geometrical conditions. Moreover, we can use the same set of random walks for barrier problems with different angles of incidence. We always set $\theta_0=0$ and rotate the boundaries as required by using, instead of cos θ and z,

$$\cos\theta' = \cos\theta\cos\alpha + \sin\theta\sin\alpha\cos\varphi$$

$$z' = x\sin\alpha + z\cos\alpha,$$

where $\alpha=\theta_0'$ is the angle of incidence.

2.2. Random Sampling

Next the sampling scheme is described, by which successive states S_n are selected, the initial state being specified as $S_0=(E_0,0,0,0,0,0)$. Calculations of a set of random walks with this initial condition will serve for the solution of problems involving monoenergetic beams of energy E_0 and arbitrary direction of incidence α. Because of the linearity of the gamma-ray diffusion equation, it is possible to obtain solutions for incident beams of specified energetic and angular composition by superposition of the results obtained with different E_0's and α's.

Prior to the discussion of the detailed steps in the sampling process, some comment is in order concerning the required random numbers. With a high-speed computer the use of tables of random numbers is clearly impractical. Instead, so-called pseudorandom numbers $r_m (0\leq r_m\leq 1)$ were used, and which were generated as required in the course of the computation by a method developed by O. Taussky-Todd [2]. They are defined by the relations

$$r_m = 2^{-42}R_m \tag{2}$$

$$R_{m+1} = 5^{17}R_m \text{ modulo } 2^{42}, \qquad R_0=1.$$

It may be shown that the period of r_m is 2^{40}, i. e., that a sequence of 2^{40} different numbers will be obtained before repetition occurs. Extensive testing carried out at the National Bureau of Standards has shown that these pseudorandom numbers satisfy the various accepted statistical criteria of randomness. It is an advantageous feature of this method that identical random walks may be recreated repeatedly for checking purposes, provided the initial random number used for the walk is recorded.

The various steps in the calculation of S_{n+1}, given S_n, follow.

a. Energy Change

The energy E_{n+1} after a scattering is determined by

$$\left[\int_{E_{n+1}}^{E_n} k(E_n,E)dE \Big/ \int_0^{E_n} k(E_n,E)dE\right] = r, \tag{3}$$

where r is a random number, and $k(E_n,E)$ is the Klein-Nishina differential coefficient (per unit path length) for Compton scattering with energy change from E_n to E.

It was found convenient to carry out the random sampling for the wavelength $\lambda=mc^2/E$, where mc^2 is the electron rest mass, rather than for the energy directly. If we make this change of variable, substitute the explicit formula for the Klein-Nishina differential coefficient, and carry out the indicated integrations, eq (3) is transformed into

$$\left\{[1-2\lambda_n(\lambda_n+1]\log\frac{\lambda_{n+1}}{\lambda_n}+\lambda_n(\lambda_n+2)\frac{\lambda_{n+1}-\lambda_n}{\lambda_{n+1}}+\lambda_n(\lambda_{n+1}-\lambda_n)+\frac{\lambda_{n+1}^2-\lambda_n^2}{2\lambda_{n+1}^2}\right\}\left\{[1-2\lambda_n(\lambda_n+1)]\log\frac{\lambda_n+2}{\lambda_n}+2\frac{1+\lambda_n}{(2+\lambda_n)^2}\right\}^{-1}=r. \tag{4}$$

To use this equation to find λ_{n+1}, given λ_n and r, would be intolerably cumbersome, even when an automatic computer is used. Latter and Kahn [3] evaluated eq (4) numerically and presented a table of $\lambda_{n+1}=\lambda_{n+1}(\lambda_n,r)$ for a grid of values in the range $0\leq r\leq 1$, $0.05\leq\lambda_n\leq 10$. The tabulation has been extended to $\lambda_n=16$ and used to obtain a polynomial representation

$$\lambda_{n+1}=\sum_{i=0}^{I}\sum_{j=0}^{J}A_{ij}(\lambda_n)^i r^j. \tag{5}$$

This required extensive bivariate interpolation, which was carried out by a convenient matrix technique. This technique is described in the appendix because it does not appear in the standard literature on numerical analysis.

The following coefficient-matrices, A_{ij}, were found to give representations of λ_{n+1} accurate to 1 percent:

$0.05\leq\lambda_n<0.5$						
i	j					
	0	1	2	3	4	5
0	0	0.1180	−0.9844	4.683	−6.896	5.079
1	1.0	.07930	20.57	−69.56	117.2	−68.29
2	0	2.124	−63.66	209.7	−342.3	194.1
3	0	−3.418	70.31	−227.8	359.2	−198.3

$0.5\leq\lambda_n<10.0$						
i	j					
	0	1	2	3	4	5
0	0	0.04100	2.851	−8.346	13.37	−5.916
1	1.0	.4779	−1.502	4.863	−5.168	1.330
2	0	−.05409	0.07590	−0.1713	−0.02945	0.1789
3	0	.002153	.0008490	−.0077	.02359	−.01891

$10 \leq \lambda_n \leq 16$				
i	j			
	0	1	2	3
0	0	27.4295	−96.6375	71.2080
1	1.0	−6.173625	23.35	−17.17
2	0	0.4584375	−1.763	1.304
3	0	−.01106	0.04342	0.03233

b. Change of Direction

Deflection and wavelength shift are related by the Compton equation

$$\cos \omega_n = 1 - \lambda_{n+1} + \lambda_n, \tag{6}$$

where ω_n is the angle between the directions of motion immediately before and after the $n+1$st scattering.

The direction of the scattered photon depends on ω_n and on an azimuth angle χ_n, which is a random quantity distributed uniformly between 0 and 2π. We need the sine and cosine of χ_n rather than χ_n itself. Hence we take advantage of the following convenient computational scheme suggested by Von Neumann [4]. Choose random numbers a and b satisfying the condition $a^2+b^2 \leq 1$, and let c be a random number that is equal to ± 1 with probability 1/2. Then

$$\cos \chi_n = \frac{2abc}{a^2+b^2} \text{ and } \sin \chi_n = \frac{a^2-b^2}{a^2+b^2}. \tag{7}$$

From the deflections ω_n and χ_n, the new angular coordinates are then determined by the following trigonometric relationships:

$$\left.\begin{aligned} &\cos \theta_{n+1} = \cos \theta_n \cos \omega_n + \sin \theta_n \sin \omega_n \cos \chi_n \\ &\sin (\phi_{n+1} - \phi_n) = \frac{\sin \chi_n \sin \omega_n}{\sin \theta_{n+1}} \\ &\cos (\phi_{n+1} - \phi_n) = \frac{\cos \omega_n - \cos \theta_n \cos \theta_{n+1}}{\sin \theta_n \sin \theta_{n+1}}. \end{aligned}\right\} \tag{8}$$

c. Displacement

The position of the $(n+1)$st scattering is defined by

$$\left.\begin{aligned} x_{n+1} &= x_n - \frac{\sin \theta_n \cos \varphi_n}{\mu_s(E_n)} \log r \\ y_{n+1} &= y_n - \frac{\sin \theta_n \sin \varphi_n}{\mu_s(E_n)} \log r \\ z_{n+1} &= z_n - \frac{\cos \theta_n}{\mu_s(E_n)} \log r \end{aligned}\right\}, \tag{9}$$

where r is a random number, and

$$\mu_s(E_n) = \int_0^{E_n} k(E_n, E)\, dE.$$

3. The Transmission-Reflection Boundary Problem

3.1. Summation Over the Collision Density [5]

The information obtained by sampling J photon random walks is contained in the set of state vectors $S_n(j)(n=0,1,\cdots L_j;\, j=1,2,\cdots J)$, which describe the state of the jth photon immediately after its nth scattering. We consider these vectors to form a set of representative points (a sample collision density) in a six-dimensional collision-density space. The solution of boundary problems can be obtained by performing appropriate sums over the collision density.

In the reflection-transmission problem, one considers a plane-parallel barrier between the planes $z=0$ and $z=t$. A beam of photons is assumed to be incident on the face $z=0$.

Reflected and transmitted radiation will be classified according to energy and direction.[6] Let R_{ik} denote the average number of photons per incident photon that are reflected from the face $z=0$ with energies in the ith interval and directions in the kth interval. Similarly, let T_{ik} denote the average number of photons transmitted through the face $z=t$. R_{ik} and T_{ik} are obtained by summations over the sample collision density as follows:

$$R_{ik} = \frac{1}{J} \sum_{j=1}^{J} \sum_{n=0}^{L_j} B_n(j) P_n(j) Q_n(j,0) f_n^{ik}(j). \tag{10}$$

The factors in this formula have the following meaning:

(a) The factor $B_n(j)$ takes into account the boundary conditions. It is equal to unity when the inequalities $0 \leq z_m(j) \leq t$ are satisfied for $m=0,1,\cdots n$, and zero otherwise. In other words, a contribution to the reflected radiation is obtained only if the photon in the state under consideration has not previously gone out of the barrier.

(b) The factor

$$P_n(j) = \prod_{m=0}^{n-1} \exp\left\{ -\frac{\sec \theta_m(j)}{\mu_A[E_m(j)]} [z_{m+1}(j) - z_m(j)] \right\} \tag{11}$$

is the probability that the photon has not been absorbed in the jth history prior to reaching state $S_n(j)$. (μ_A is the absorption coefficient.)

(c) The quantity $Q_n(j,z')$ denotes the probability that a photon starting from state $S_n(j)$ will cross the plane $z=z'$ without further scattering or absorption. It is defined as follows:

$Q_n(j,z')$ vanishes except when $\sec \theta_n(j)[z'-z_n(j)] \geq 0$, in which case

$$Q_n(j,z') \exp\left\{ -\frac{\sec \theta_n(j)}{\mu[E_n(j)]} [z' - z_n(j)] \right\} \tag{12}$$

[5] The method described in this section is closely related to suggestions by H. Kahn, [3].

[6] 32 energy intervals and 10 angular intervals have been used.

($\mu = \mu_A + \mu_s$ is the total linear attenuation coefficient).

(d) $f_n^{ik}(j)$ is the energy-angle classification factor. It is equal to unity when $E_n(j)$ is in the ith energy interval and $\theta_n(j)$ in the kth angular interval, and zero otherwise.

Transmitted radiation T_{ik} is calculated by a formula similar to eq (10) but with $Q_n(j,0)$ replaced by $Q_n(j,t)$.

We shall use the collision density also for the evaluation of the flux in an infinite medium in which a plane source is embedded in the plane $z=0$. By comparing the results for this problem with those for the barrier, the nature of the boundary effect can be established. Moreover, the Monte Carlo results for the infinite medium can be checked against those obtained by systematic moment-method calculations. Such a comparison is of use in establishing the validity and accuracy of the random-sampling approach. Let $B_{ik}(z')$ denote the average number of photons crossing the plane $z=z'$ from both directions (our main interest will be in the planes that form the barrier boundaries: $z'=0$ and $z'=t$). The necessary summation over the collision density is similar to formula (10), except that the boundary factor $B_n(j)$ is omitted.

When the sampled collision density is used for the simultaneous determination of R_{ik}, T_{ik}, $B_{ik}(0)$, and $B_{ik}(t)$, all states $S_n(j)$ make a contribution to the final score except those for which $z_n(j)<0$ and $\cos\theta_n(j)<0$, or $z_n(j)>t$ and $\cos\theta_n(j)>0$. This is in contrast to a direct stochastic analogue method, which would allow only those sections of the random walks containing an actual crossing of the boundaries to contribute to the score. The more elaborate scoring procedure gives proper credit for "near misses," i. e., collisions taking place close to a boundary, for which the factor $Q_n(j,z')$ is very close to unity.

3.2. Fluxes and Buildup Factors

The SEAC calculation is designed to yield the quantities R_{ik}, T_{ik}, and B_{ik}, which represent the average number of photons crossing the planes $z=0$ and $z=t$ per unit area (the number flux). Radiation detectors often do not measure the number flux directly, so that it is desirable to calculate various related types of flux. These can all be obtained from the number flux through multiplication by suitable weight factors, depending on the energy and direction of the photons. For example, multiplication of the number flux by the average energy, $\langle E_i\rangle$, yields the energy flux, division by the average value, absolute value $|\langle\cos\theta_k\rangle|$, yields fluxes through a unit area whose normal is in the direction of motion of the radiation. This is the flux that a nondirectional detector would measure. Some inaccuracy is introduced into these flux-conversions because the averages $\langle E_i\rangle$ and $\langle\cos\theta_k\rangle$ are to some extent arbitrary. Arithmetic means have been used.

According to the usage common in shielding calculations the results for the total flux (integrated over-all directions and spectral energies) are presented in the form of buildup factors, defined as the ratio of the total to the unscattered flux [5]. For the various types of flux described above, the buildup factors for an infinite homogenous medium have the following form:

Number buildup factors

$$B_N = \sum_{ik} B_{ik} / \exp(-\mu_0 z/\cos\alpha)$$

$$B'_N = \sum_{ik} \frac{B_{ik}}{|\langle\cos\theta_k\rangle|} \Bigg/ \frac{\exp(-\mu_0 z/\cos\alpha)}{\cos\alpha} \tag{13}$$

Energy buildup factors

$$B_E = (\sum_{ik} \langle E_i\rangle B_{ik} / E_0 \exp(-\mu_0 z/\cos\alpha)$$

$$B'_E = \sum_{ik} \langle E_i\rangle \frac{B_{ik}}{|\langle\cos\theta_k\rangle|} \Bigg/ \frac{E_0}{\cos\alpha} \exp(-\mu_0 z/\cos\alpha), \tag{14}$$

where μ_0 is the total attenuation coefficient of the source radiation, and z is the distance between the source plane and the plane of observation. In order to obtain the corresponding buildup factors T_N, T'_N, T_E, and T'_E, one replaces B_{ik} in eq (13) and (14) by T_{ik}, and z by the barrier thickness, t. The reflection buildup factors R_N, R'_N, R_E, and R'_E are obtained by using R_{ik} and setting $z=0$.

4. Results[7]

4.1. Energy Spectra

In figures 1, a, b, c, and d, energy spectra are shown in histogram form for the number flux of photons reflected and transmitted by barriers, reflected by a semi-infinite medium, and for the flux in an infinite medium through planes that correspond to the barrier boundary planes. The histograms pertain to scattered radiation only.[8] Spectra are shown for normal incidences ($\alpha=0°$) and for oblique incidence ($\alpha=60°$). The oblique barrier thickness is the same for both cases: $(\mu_0 t/\cos\alpha)=2$. The shaded areas between the "finite slab" and the "infinite medium" histograms are a measure of the boundary effect. It can be seen that the boundaries greatly reduce the amount of soft radiation below 200 kev. The reason for this is that in an infinite medium soft radiation is mainly due to photons that have overshot the boundary plane and have been turned around in a collision in the close vicinity of the boundary, making their second passage through the boundary with resultant low energy.

[7] Based on the analysis of 400 random walks for each problem.

[8] To obtain the scattered flux only, one must begin the sum in eq (10) with $n=1$.

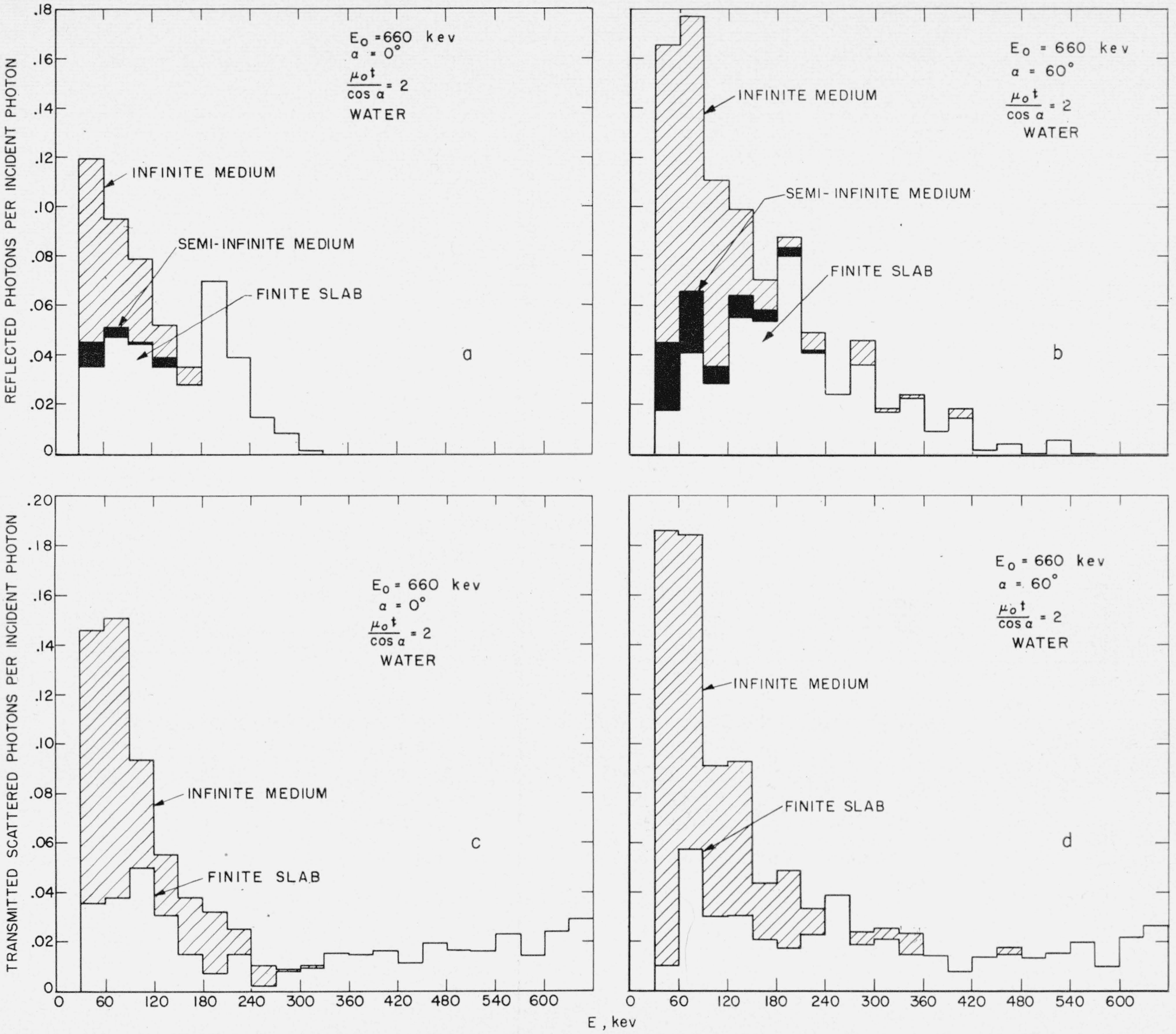

FIGURE 1. *Energy spectra of photons reflected and transmitted by water barriers and of photons in an infinite homogenous medium crossing planes corresponding to the barrier boundaries.*

The spectra pertain to a monodirectional beam of 0.66-Mev photons incident on the barrier (or released within a semi-infinite medium) with obliquity α.
a, Reflection; obliquity $\alpha=0°$ (normal incidence); b, Reflection; obliquity $\alpha=60°$; c, Transmission; obliquity $\alpha=0°$ (normal incidence); d, Transmission; obliquity $\alpha=60°$.

4.2. Angular Distributions

Figure 2, a, shows the angular distribution of the reflected number flux from a barrier with oblique thickness $\mu_0 t=1$, and from a semi-infinite medium for obliquity angles of incidence $\alpha=0°$ and $\alpha=60°$. Figure 2, b, shows the angular spectra of transmitted scattered photons for normal incidence and barrier thickness $\mu_0 t=1$ and $\mu_0 t=4$.

4.3. Buildup Factors

The various buildup factors for transmission, reflection, and an infinite medium (as defined in section 3.1 and 3.2) are listed in table 1 for the number flux, and in table 2 for the energy flux for 0.66-Mev radiation in water. Estimated standard deviations are indicated, which were obtained by dividing the 400 photon histories into groups of 50 each and computing the dispersion of the buildup factors obtained for the various groups.

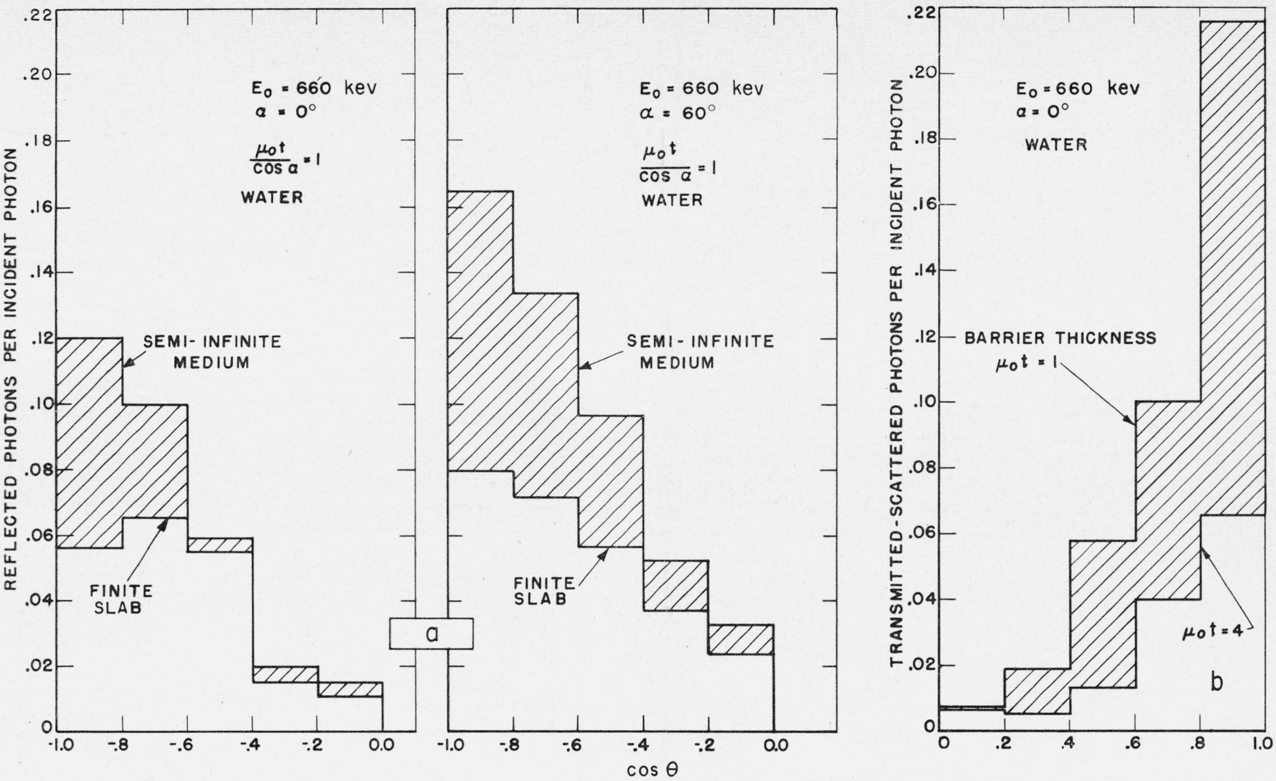

FIGURE 2. *Angular distributions of photons reflected and transmitted by water barriers.*

The distributions pertain to a monodirectional beam of 0.66-Mev photons incident on the barrier with obliquity α.
a, Reflection; obliquities $\alpha=0°$ and 60°; b, Transmission; obliquity $\alpha=0°$ (normal incidence).

TABLE 1. *Number buildup factors for 0.66-Mev radiation in water*

α	$\frac{\mu_0 t}{\cos \alpha}$	R_N	R'_N	T_N	T'_N	B_N	B'_N
°							
0	0	------	------	------	------	1.61 ±0.09	2.30 ±0.16
0	1	1.18 ±0.03	1.36 ±0.05	2.09 ±0.16	2.73 ±0.18	3.69 ±0.26	6.24 ±0.35
0	2	1.29 ±0.03	1.55 ±0.06	3.94 ±0.45	6.02 ±0.55	7.11 ±0.64	12.3 ±1.3
0	4	1.31 ±0.05	1.59 ±0.07	8.21 ±1.75	13.5 ±2.2	13.3 ±2.8	24.3 ±4.2
0	∞	1.31 ±0.05	1.61 ±0.07	------	------	------	------
60	0	------	------	------	------	1.85 ±0.11	1.97 ±0.13
60	1	1.27 ±0.05	1.30 ±0.06	2.00 ±0.13	2.17 ±0.13	4.13 ±0.25	4.41 ±0.28
60	2	1.41 ±0.06	1.48 ±0.07	4.13 ±0.46	3.90 ±0.50	8.89 ±0.95	8.21 ±0.98
60	4	1.47 ±0.06	1.53 ±0.07	15.4 ±2.0	14.2 ±2.5	29.3 ±4.9	30.2 ±5.3
60	∞	1.48 ±0.06	1.53 ±0.07	------	------	------	------

TABLE 2. *Energy buildup factors for 0.66-Mev radiation in water*

α	$\frac{\mu_0 t}{\cos \alpha}$	R_E	R'_E	T_E	T'_E	B_E	B'_E
°							
0	0	------	------	------	------	1.10 ±0.02	1.23 ±0.04
0	1	1.05 ±0.01	1.10 ±0.02	1.62 ±0.06	1.89 ±0.09	1.87 ±0.07	2.48 ±0.10
0	2	1.07 ±0.02	1.14 ±0.03	2.50 ±0.20	3.21 ±0.30	2.97 ±0.22	4.07 ±0.31
0	4	1.07 ±0.02	1.15 ±0.03	3.62 ±0.39	5.64 ±0.65	4.33 ±0.39	6.98 ±0.72
0	∞	1.07 ±0.02	1.15 ±0.03	------	------	------	------
60	0	------	------	------	------	1.19 ±0.03	1.23 ±0.04
60	1	1.10 ±0.03	1.11 ±0.05	1.57 ±0.07	1.65 ±0.09	1.98 ±0.09	2.15 ±0.10
60	2	1.13 ±0.03	1.17 ±0.05	2.43 ±0.22	2.37 ±0.20	3.24 ±0.25	3.48 ±0.29
60	4	1.14 ±0.03	1.18 ±0.05	5.92 ±0.68	5.40 ±0.73	7.61 ±0.91	6.21 ±1.05
60	∞	1.14 ±0.03	1.18 ±0.05	------	------	------	------

5. Discussion

The results presented have a preliminary character. Greater sample sizes are desirable, as well as the extension of the calculation to other energies and media. Moreover, the scoring method used is not expected to be very successful for penetrations of depth $\mu_0 t > 4$ because excessively large sample sizes would be required. Prior to extending the calculations by the collision-density method, other Monte Carlo approaches have been explored, including a semianalytic method designed for dealing with deep as well as shallow penetrations [6]. Table 3 gives a comparison of the buildup factors obtained in this investigation (a) with those found by the semianalytical Monte Carlo method, (b) with the Monte Carlo results of a group at the Naval Research Laboratory [7], and (c), for an infinite medium, with calculations carried out according to the moment method of Spencer and Fano [1, 8]. The agreement is generally good, indicating that the shallow penetration of gamma radiation, in the presence of boundaries, can be calculated accurately by the Monte Carlo method. The results for R_N and R_E at 0.66 Mev are consistent with the results of a Monte Carlo calculation at 1 Mev by Hayward and Hubbell [9].

TABLE 3. *Comparison of buildup factors obtained in various calculations for 0.66-Mev radiation in water*

Column 1, this paper; 2, semianalytic Monte Carlo method [6]; 3, Monte Carlo, NRL [7]; 4, Spencer-Fano moment method [8].

	α	$\frac{\mu_0 t}{\cos\alpha}$	Method			
			1	2	3	4
R'_N	0°	∞	1.53	------	1.59	------
T'_N	------	1	2.73	------	2.74	------
		2	6.02	------	6.60	------
		4	13.5	------	13.0	------
B'_N	------	1	6.24	------	6.0	------
		2	12.3	------	12.3	------
		4	24.3	------	25.0	------
R'_E	------	∞	1.15	1.15	1.14	------
T'_E	------	1	1.89	1.96	1.92	------
		2	3.21	3.06	3.30	------
		4	5.64	5.99	5.55	------
B'_E	------	0	1.23	------	------	1.30
		1	2.48	2.44	2.43	2.43
		2	4.07	4.02	3.75	3.89
		4	6.98	7.15	6.55	7.37
B'_E	60°	0	1.23	------	------	1.27
		1	2.15	------	------	2.05
		2	3.48	------	------	3.28
		4	6.21	------	------	7.82

6. References

[1] L. V. Spencer and U. Fano, J. Research, NBS **46,** 446 (1951) RP2213.

[2] H. A. Meyer, L. S. Gephart, and N. L. Rasmussen, On the generation and testing of random digits, WADC Technical Report 54–55 (1954).

[3] R. Latter and H. Kahn, Rand Report R–170 (1949).

[4] Monte Carlo Methods, NBS Applied Math. Series (1951) AMS12.

[5] H. Goldstein and J. E. Wilkins, Jr., AEC Report NYO-3075, (June 1954).

[6] M. J. Berger and J. Doggett, J. Research NBS (publication pending).

[7] L. A. Beach, R. B. Theus, J. D. Plawchan, and W. R. Faust, NRL Report 4412 (1954).

[8] M. J. Berger, J. Research NBS (publication pending).

[9] E. Hayward and J. Hubbell, Phys. Rev. **93,** 955 (1954).

[10] A. C. Aitken, Determinants and matrices, p. 118, (Interscience Publishers, Inc., New York, N. Y., 1951).

7. Appendix. A Method of Bivariate Interpolation

Suppose we know a bivariate function $f(p,q)$ at $(M+1)(N+1)$ gridpoints (p_s,q_t) $(s=0,1, \ldots, M;$ $t=0,1, \ldots, N)$. The problem is to use this knowledge for determining the expansion coefficients in a polynomial expansion

$$f(p,\,q)=\sum_{i=0}^{M}\sum_{j=0}^{N} A_{ij}p^i q^j. \tag{17}$$

Let $F=f(p_s,q_t)$ be the known matrix of functional values, and $A=(A_{ij})$ the desired coefficient matrix. From the variables p and q we form the matrices $P=(p_s)^i$ and $Q=(q_t)^i$. In matrix form, eq (17) becomes

$$F=PAQ', \tag{18}$$

where Q′ is the transpose of Q. Hence

$$A=P^{-1}F(Q^{-1})'. \tag{19}$$

P and Q are so-called alternant matrices whose inverse is well known [10]. The prescription for obtaining the inverse is simplest to describe by means of an example. When P has rank 3

$$\begin{pmatrix} 1 & p_0 & p_0^2 \\ 1 & p_1 & p_1^2 \\ 1 & p_2 & p_2^2 \end{pmatrix}^{-1} = \begin{pmatrix} \dfrac{p_1p_2}{(p_0-p_1)(p_0-p_2)} & \dfrac{p_0p_3}{(p_1-p_0)(p_1-p_2)} & \dfrac{p_0p_1}{(p_2-p_0)(p_2-p_1)} \\[2ex] \dfrac{-(p_1+p_2)}{(p_0-p_1)(p_0-p_2)} & \dfrac{(p_0+p_2)}{(p_1-p_0)(p_1-p_2)} & \dfrac{-(p_0+p_1)}{(p_2-p_0)(p_2-p_1)} \\[2ex] \dfrac{1}{(p_0-p_1)(p_0-p_2)} & \dfrac{1}{(p_1-p_0)(p_1-p_2)} & \dfrac{1}{(p_2-p_0)(p_2-p_1)} \end{pmatrix}. \tag{20}$$

The numerators of of the elements in the respective columns are elementary symmetric functions in the arguments p_0, p_1, and p_2, with one argument omitted each time. The arrangement of the denominators is obvious.

When the grid points are equidistant, one can, without loss of generality, set $p_s=s$. The inverses P^{-1} for this case are listed below for the first few alternant matrices:

The sum of the elements in the first row of each inverse matrix is 1, and the sum of the elements in each other row is zero. This is also true for the case of nonequidistant grid points, and provides a useful arithmetical check.

The author thanks Frank Stockmal for his help in coding the problem for SEAC, and Mary Orr and John Doggett for their assistance with the hand computations.

$$\begin{pmatrix} 1 & 0 \\ -1 & 1 \end{pmatrix} \quad \frac{1}{2}\begin{pmatrix} 2 & 0 & 0 \\ -3 & 4 & 1 \\ 1 & -2 & 1 \end{pmatrix} \quad \frac{1}{6}\begin{pmatrix} 6 & 0 & 0 & 0 \\ -11 & 18 & -9 & 2 \\ 6 & -15 & 12 & -3 \\ -1 & 3 & -3 & 1 \end{pmatrix} \quad \frac{1}{24}\begin{pmatrix} 24 & 0 & 0 & 0 & 0 \\ -50 & 96 & -72 & 32 & -6 \\ 35 & -104 & 114 & -56 & 11 \\ -10 & 36 & -48 & 28 & -6 \\ 1 & -4 & 6 & -4 & 1 \end{pmatrix}$$

$$\frac{1}{120}\begin{pmatrix} 120 & 0 & 0 & 0 & 0 & 0 \\ -274 & 600 & -600 & 400 & -150 & 24 \\ 225 & -770 & 1070 & -780 & 305 & -50 \\ -85 & 355 & -590 & 490 & -205 & 35 \\ 15 & -70 & 130 & -120 & 55 & -10 \\ 1 & 5 & -10 & 10 & -5 & 1 \end{pmatrix}$$

WASHINGTON, May 10, 1955.